International Scholarly Research Network
ISRN Ceramics
Volume 2012, Article ID 876123, 5 pages
doi:10.5402/2012/876123

Research Article

Rietveld Structure Refinement and Cation Distribution of Cr^{3+} Substituted Nanocrystalline Ni-Zn Ferrites

A. A. Birajdar,[1] Sagar E. Shirsath,[2] R. H. Kadam,[3] S. M. Patange,[3] D. R. Mane,[2] and A. R. Shitre[4]

[1] *Department of Physics, SMP College, Murum, Osmanabad 413605, India*
[2] *Spin Device Technology Center, Faculty of Engineering, Shinshu University, Nagano 380-8553, Japan*
[3] *Materials Research Laboratory, Shrikrishna Education Society's Srikrishna Mahavidyalaya, Gunjoti, Omerga, Osmanabad 413613, India*
[4] *Department of Physics, YC College, Tuljapur, Osmanabad 413 601, India*

Correspondence should be addressed to Sagar E. Shirsath, shirsathsagar@hotmail.com

Received 7 April 2012; Accepted 10 July 2012

Academic Editors: M. A. Schiavon and W. Tseng

Ferrite nanoparticles of $Ni_{0.7}Zn_{0.3}Cr_xFe_{2-x}O_4$ were prepared by a sol-gel autocombustion method. The prepared samples were shown to have a cubic spinel structure by applying the full pattern fitting of the Rietveld method. The unit cell dimension, discrepancy factor, and interatomic distance have been determined. As the Cr^{3+} content x increases, the unit cell dimensions and crystallite size are decreased. The IR spectra show two absorption bands in the wave number range of 400 to 600 cm^{-1}.

1. Introduction

Ni-Zn ferrites are one of the most versatile soft magnetic materials. Recently, the technological application of these materials has been studied extensively, primarily due to their applicability in many electronic devices owing to their high permeability at high frequency, remarkably high-electrical resistivity, low-eddy current loss, and reasonable cost [1–3]. The Ni-Zn ferrite is a well-known mixed inverse spinel, whose unitary cell is represented by the formula $(Zn_xFe_{1-x})[Ni_{1-x}Fe_{1+x}]O_4$ [4]. The addition of impurities induces changes in the defect structure and texture of the crystal [5], creating significant modifications in the magnetic and electrical properties of these materials. Nickel chromate is a normal spinel while nickel ferrites are inverse spinels. To determine unit cell dimension imperfections and their nature to find the reason for the phase transformation of the synthesized material, X-ray characterization techniques based on structure and microstructure refinement are usually preferred [6, 7]. Rietveld analysis based on structure and microstructure refinement [8, 9] has been adopted in the present study for precise determination of several microstructural parameters. The aim of the present work is to study the structure refinement by the Rietveld method and the study of cation distribution of chromium substituted Ni-Zn ferrites prepared by a sol-gel method.

2. Experimental

The ferrite powders with a generic formula $Ni_{0.7}Zn_{0.3}Cr_xFe_{2-x}O_4$ (where $x = 0.0$–0.5, in the step of 0.1) were synthesized by the sol-gel auto-combustion method using the AR grade citric acid ($C_6H_8O_7 \cdot H_2O$), nickel nitrate ($Ni(NO_3)_2 \cdot 6H_2O$), zinc nitrate ($Zn(NO_3)_2 \cdot 6H_2O$), chromium nitrate ($Cr(NO_3)_3 \cdot 9H_2O$), and iron nitrate ($Fe(NO_3)_3 \cdot 9H_2O$). The as-prepared powders of all the samples were sintered at 600°C for 4 h to get the final product. Details of the sol-gel combustion technique procedure have been reported in our previous publications [10, 11]. The samples were X-ray examined by Phillips X-ray diffractometer (Model 3710) with $Cu - K_\alpha$ radiation ($\lambda = 1.5405$Å). The data were processed to analyze all of the samples using the computer Program FullProf.2k

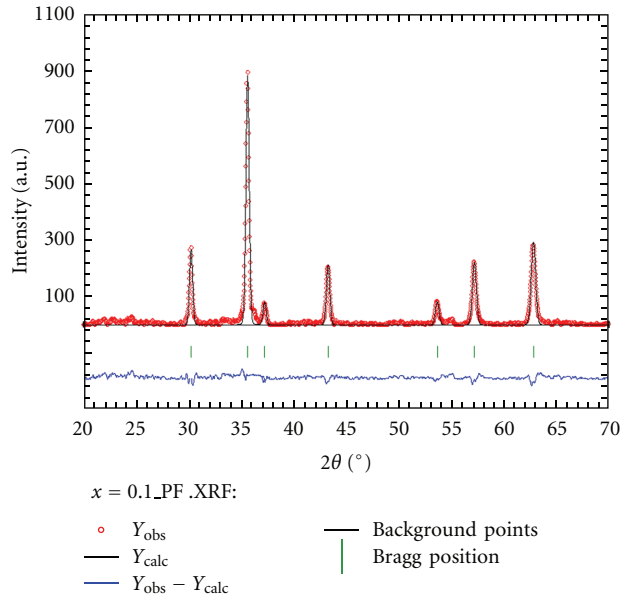

Figure 1: Rietveld refined X-ray diffraction pattern of $x = 0.1$.

(Version 4.30—Apr, 2008-ILL JRC) in the Rietveld method for structure refinement. Program refinement of the first samples was started with the space group Fd3m, origin at −3 m, O in 32e$^-$, A site in 8f, and B site in 16c. In the first step the global parameters, such as 2θ-zero and background, were refined. In the next step, the structural parameters, such as lattice parameter, atomic coordinates, and site occupancy, were refined. IR spectra were recorded in the range 350–800 cm^{-1} at room temperature by an IR spectrometer (Bruker).

3. Results and Discussion

The XRD patterns confirm the single phase cubic spinel structure, and XRD refinement was continuous until convergence was reached with a goodness factor very close to 1. The values of the discrepancy factor (R_{wp}), expected values (R_{exp}), and Bragg value (R_{Bragg}) with the goodness of fit index (x^2) are listed in Table 1, our Rietveld refined values are in good agreement with the literature report for other ferrite systems [12, 13]. Figure 1 represents the typical Rietveld refined X-ray pattern for sample $x = 0.1$. The lattice constant calculated by the Rietveld method and the values are listed in Table 1. The lattice constant initially increases and then begins to decrease, the initial increase of the lattice constant from $x = 0.0$ to 0.2 may be due to the fact that the substitution of Cr^{3+} up to $x = 0.2$ does not affect the lattice. The decrease in the lattice constant above $x > 0.2$ is related to the difference in ionic radii of Fe^{3+} and Cr^{3+}. In the present ferrite system, Fe^{3+} ions (0.67 Å) ions are replaced by the relatively small Cr^{3+} ions (0.64 Å). The system $Ni_{0.7}Zn_{0.3}Cr_xFe_{2-x}O_4$ under investigation is neither completely normal nor completely inverse. We have previously reported similar behavior of

Table 1: Discrepancy factor (R_{wp}), expected values (R_{exp}), goodness fit factor (χ^2), lattice constant (a), and crystallite size (t) of $Ni_{0.7}Zn_{0.3}Fe_{2-x}Cr_xO_4$.

Comp. x	R_{wp} (%)	R_{exp} (%)	χ^2	a (Å)	t (nm)
0.0	6.24	2.91	2.14	8.366	35
0.1	7.32	3.70	1.98	8.370	32
0.2	8.84	3.94	2.24	8.375	29
0.3	4.58	2.49	1.84	8.363	25
0.4	5.48	2.74	2.00	8.351	22
0.5	6.48	3.30	1.96	8.336	20

lattice constant with Cr^{3+} content x [14]. The average crystallite size (t) was determined using the line broadening of the most intense (311) diffraction peak using the Debye-Scherrer formula [15]. The values of the crystallite size are given in Table 1. The crystallite size decreases from 35 nm to 20 nm with increasing Cr content.

The cation distribution in spinel ferrite can be obtained from an analysis of the X-ray diffraction pattern. In the present work, the Rietveld refinement method [8] and Bertaut method [16] are used to determine the cation distribution. The best information on cation distribution is achieved by comparing the experimental and calculated intensity ratios for reflections whose intensities (i) are nearly independent of the oxygen parameter, (ii) vary with the cation distribution in opposite ways, and (iii) do not significantly differ. The final results of cation distribution obtained from the Rietveld refinement and the analysis of X-ray diffraction and are given in Tables 2 and 3, respectively. In these tables, the fraction of Fe^{3+} ions in either site is listed. The results demonstrate that Ni^{2+} ions occupy B sites, whereas Zn^{2+} ions occupy tetrahedral A sites. Cr^{3+} preferentially replaces Fe^{3+} from octahedral sites because of favorable crystal-field effects ($Cr^{3+}6/5\Delta_0$, $Cr^{3+}0\Delta_0$) [17]. The data in Tables 2 and 3 shows that Cr^{3+} ions predominately occupy the octahedral sites, which is consistent with the preference for large octahedral-site energy. With increasing Cr^{3+} content, the fraction Cr^{3+} ions in octahedral sites increases, whereas the fraction of Fe^{3+} ions in octahedral sites decreases linearly.

Using the values of a, the radius of oxygen ion $R_O = 1.32$ Å, and radius of tetrahedral A site (r_A) in the following expression, the oxygen positional parameter u can be calculated [18]

$$u = \left[(r_A + R_O) \frac{1}{\sqrt{3}a} + \frac{1}{4} \right]. \quad (1)$$

Table 3 shows the increasing value of the oxygen positional parameter from 0.3888 to 0.3893 Å. In most oxide spinels, the oxygen ions are larger than the metallic ions. In spinel-like structures, the oxygen positional parameter has a value near 0.375 Å, for which the arrangement of O^{2-} ions is equal, exactly a cubic closed packing, but in an actual spinel lattice, this ideal pattern is slightly deformed.

Table 2: Values of atomic coordinates (x, y, z), occupancy (g), and degree of inversion (δ) of $Ni_{0.7}Zn_{0.3}Fe_{2-x}Cr_xO_4$.

Atom	$x = 0.0$		$x = 0.1$		$x = 0.2$		$x = 0.3$		$x = 0.4$		$x = 0.5$	
	$x = y = z$	g	$x = y = z$	g	$x = y = z$	g	$x = y = z$	g	$x = y = z$	g	$x = y = z$	g
O	0.252	4.000	0.2532	4.0000	0.2542	4.0000	0.2572	4.000	0.2542	4.000	0.2456	4.000
Ni	0.500	0.700	0.5000	0.7000	0.5000	0.7000	0.5000	0.700	0.5000	0.700	0.5000	0.700
Zn	0.500	0.010	0.5000	0.0125	0.5000	0.0145	0.5000	0.000	0.5000	0.000	0.5000	0.000
Cr	0.500	0.000	0.5000	0.1000	0.5000	0.2000	0.5000	0.300	0.5000	0.400	0.5000	0.500
Fe	0.500	1.290	0.5000	1.1875	0.5000	1.0855	0.5000	1.000	0.5000	0.900	0.5000	0.800
Ni	0.125	0.000	0.1250	0.0000	0.1250	0.0000	0.1250	0.000	0.1250	0.000	0.1250	0.000
Zn	0.125	0.290	0.1250	0.2875	0.1250	0.2855	0.1250	0.300	0.1250	0.300	0.1250	0.300
Cr	0.125	0.000	0.1250	0.0000	0.1250	0.000	0.1250	0.000	0.1250	0.000	0.1250	0.000
Fe	0.125	0.710	0.1250	0.7125	0.1250	0.7145	0.1250	0.700	0.1250	0.700	0.1250	0.700
δ	0.8466		0.8244		0.7648		0.5264		0.4256		0.3244	

Table 3: Cation distribution and oxygen positional parameter (u) of $Ni_{0.7}Zn_{0.3}Fe_{2-x}Cr_xO_4$.

Comp. x	Cation distribution	u (Å)
0.0	$(Zn_{0.3}Fe_{0.7})^A\ [Ni_{0.7}Fe_{1.3}]^B\ O_4$	0.3888
0.1	$(Zn_{0.3}Fe_{0.7})^A\ [Cr_{0.1}Ni_{0.7}Fe_{1.2}]^B\ O_4$	0.3888
0.2	$(Zn_{0.3}Fe_{0.7})^A\ [Cr_{0.2}Ni_{0.7}Fe_{1.1}]^B\ O_4$	0.3887
0.3	$(Zn_{0.3}Fe_{0.7})^A\ [Cr_{0.3}Ni_{0.7}Fe_{1.0}]^B\ O_4$	0.3889
0.4	$(Zn_{0.3}Fe_{0.7})^A\ [Cr_{0.4}Ni_{0.7}Fe_{0.9}]^B\ O_4$	0.3891
0.5	$(Zn_{0.3}Fe_{0.7})^A\ [Cr_{0.5}Ni_{0.7}Fe_{0.8}]^B\ O_4$	0.3893

u has a value of 0.37 Å when the origin is chosen on the tetrahedral sites. However, the structure is a centric and the structure factor calculation is less direct [19]. Our value of u is larger than the ideal value ($u = 0.375$ Å), which may probably be due to many reasons, including the history of the samples and experimental or measurement errors, for example, the precision of the observed X-ray intensity and the theoretical data used for the scattering model of the system. In most spinels, $u > 0.375$ is obtained because of a small displacement of the anions due to the expansion of the tetrahedral interstices. In the present work, $u > 0.375$ may be due to an anion displacement from the ideal position [20]. The lattice disturbance is confirmed by the data for the lattice constant and the oxygen positional parameter.

The infrared spectra can give some additional information on valance state and the different vibrational modes of the crystal lattice. The band position obtained from these IR spectra is given in Table 4. The IR spectra of the series $Ni_{0.7}Zn_{0.3}Cr_xFe_{2-x}O_4$ are shown in Figure 2. The high-frequency band ν_1 is in the range of 575–89 cm^{-1} and the low-frequency band ν_2 is in the range of 400–420 cm^{-1}. The absorption bands observed within this range are an indication of the formation of the single phase spinel structure. Vibrational bands ν_1 and ν_2 are assigned to the intrinsic vibration of tetrahedral and octahedral sites [21]. A small band ν_3 is observed at 493 cm^{-1} and 501 cm^{-1} for $x = 0.4$ and 0.5, respectively. Similar IR spectra have been reported in the literature for a ceramically prepared Cr substituted ferrite system [22]. It can be noticed from IR spectra that tetrahedral complex (ν_1) have more intense absorption than octahedral complex (ν_2). This is a consequence of the first selection rule: transitions between d orbitals in a complex having a center of symmetry are forbidden. As a result, absorption bands for octahedral complex are weak as compared to tetrahedral complex, the lack of centre of symmetry makes transition between d orbitals more allowed [23]. The change in band position is attributed to the change in Fe^{3+}-O^2 distance for the tetrahedral and octahedral complex. The small change in frequency of the bands ν_1 and ν_2 is due to the distribution of Cr^{3+} ions, which replace the Fe^{3+} ion only at the octahedral B site only, thus making no significant change in size of the octahedral site. Further, the decrease in the $Fe_B{}^{3+}$-$O_2{}^{2-}$ intermolecular distance increases the metal-oxygen vibrational energies, which arises from the decrease in the number of Fe^{3+}-$O_2{}^{2-}$ complexes caused by the increase of the number of Cr^{3+} - $O_2{}^{2-}$ complexes [24] and the formation of $Me^{3+}O_2{}^{2-}$ at A and B sites (Me = Ni^{2+}).

The force constant is the second derivative of the potential energy with respect to the site radius with the other independent parameters kept constant. The force constant for tetrahedral site (K_t) and octahedral site (K_o) were calculated using the method suggested by Waldron [21]. According to Waldron, the force constants K_t, and K_o for respective sites are given by

$$K_t = 7.62 \times M_1 \times \nu_1^2 \times 10^{-3}\ \text{dyne/cm},$$
$$K_o = 10.62 \times \frac{M_2}{2} \times \nu_2^2 \times 10^{-3}\ \text{dyne/cm}, \quad (2)$$

where M_1 and M_2 are molecular weight of cations on A and B sites, respectively. The bond lengths R_A and R_B have been calculated using the formula given by Gorter [25]. The

Table 4: Band positions (ν_1 and ν_2), force constants (K_o and K_t), and bond lengths (R_A and R_B) of $Ni_{0.7}Zn_{0.3}Fe_{2-x}Cr_xO_4$.

Comp. "x"	ν_1(cm^{-1})	ν_2 (cm^{-1})	$K_o \times 10^5$(dyne/cm)	$K_t \times 10^5$ (dyne/cm)	R_A (Å)	R_B (Å)
0.0	575	400	1.478	1.509	0.691	1.207
0.1	579	406	1.499	1.551	0.691	1.209
0.2	583	406	1.520	1.548	0.691	1.211
0.3	587	417	1.541	1.629	0.691	1.206
0.4	588	418	1.546	1.633	0.691	1.201
0.5	589	420	1.551	1.645	0.691	1.194

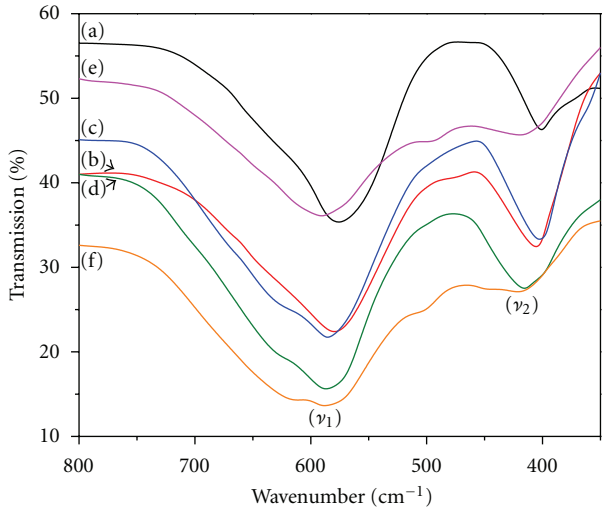

Figure 2: Infrared spectroscopy of all the samples of $Ni_{0.7}Zn_{0.3}Cr_xFe2-_xO^4$, (a) $x = 0.0$, (b) $x = 0.1$, (c) $x = 0.2$, (d) $x = 0.3$, (e) $x = 0.4$, and (f) $x = 0.5$.

molecular weights of the tetrahedral M_1 and octahedral M_2 sites have been calculated using the cation distribution data in Table 3. The values of R_A, R_B the force constants K_t and K_o are listed in Table 4. The force constants K_t and K_o are found to increase, whereas R_B initially increases and then decreases with Cr content. It is an established fact in IR studies that the force constant is inversely proportional to the bond length [26].

4. Conclusions

In conclusion, the substitution of Cr^{3+} has induced significant changes in the structural properties of Ni-Zn ferrite. Experimental results revealed that the lattice constant and cell volume decrease with increasing Cr^{3+} content in Ni-Zn ferrite. The cation distribution suggests that Cr^{3+} and Zn^{2+} both have a strong preference towards the octahedral B site and that Ni^{2+} also occupies the B site, whereas Fe^{3+} occupies both the A and B sites. The IR spectra confirm the formation of the spinel structure and give the distribution of ions between A and B sites.

References

[1] A. Goldman, *Modern Ferrite Technology*, Springer, New York, NY, USA, 2nd edition, 2006.

[2] R. V. Mangalaraja, S. Ananthakumar, P. Manohar, and F. D. Gnanam, "Initial permeability studies of Ni-Zn ferrites prepared by flash combustion technique," *Materials Science and Engineering A*, vol. 355, no. 1-2, pp. 320–324, 2003.

[3] Y. Wang, F. Xu, L. Li, H. Liu, H. Qiu, and J. Jiang, "Magnetic properties of La-substituted Ni-Zn-Cr ferrites via rheological phase synthesis," *Materials Chemistry and Physics*, vol. 112, no. 3, pp. 769–773, 2008.

[4] R. C. O'Handley, *Modern Magnetic Materials-Principles and Applications*, Wiley-IEEE Press, New York, NY, USA, 2000.

[5] S. E. Shirsath, S. S. Jadhav, B. G. Toksha, S. M. Patange, and K. M. Jadhav, "Remarkable influence of Ce^{4+} ions on the electronic conduction of $Ni_{1-2x}Ce_xFe_2O_4$," *Scripta Materialia*, vol. 64, no. 8, pp. 773–776, 2011.

[6] S. M. Patange, S. E. Shirsath, G. S. Jangam, K. S. Lohar, S. S. Jadhav, and K. M. Jadhav, "Rietveld structure refinement, cation distribution and magnetic properties of Al3+ substituted NiFe2O4 nanoparticles," *Journal of Applied Physics*, vol. 109, no. 5, Article ID 053909, 2011.

[7] S. K. Pradhan, S. Bid, M. Gateshki, and V. Petkov, "Microstructure characterization and cation distribution of nanocrystalline magnesium ferrite prepared by ball milling," *Materials Chemistry and Physics*, vol. 93, no. 1, pp. 224–230, 2005.

[8] H. M. Rietveld, "Line profiles of neutron powder-diffraction peaks for structure refinement," *Acta Crystallographica*, vol. 22, pp. 151–152, 1967.

[9] R. A. Young and D. B. Wiles, "Profile shape functions in Rietveld refinements," *Journal of Applied Crystallography*, vol. 15, pp. 430–438, 1982.

[10] S. E. Shirsath, B. G. Toksha, R. H. Kadam et al., "Doping effect of Mn2 on the magnetic behavior in NiZn ferrite nanoparticles prepared by solgel auto-combustion," *Journal of Physics and Chemistry of Solids*, vol. 71, no. 12, pp. 1669–1675, 2010.

[11] D. R. Mane, D. D. Birajdar, S. Patil, S. E. Shirsath, and R. H. Kadam, "Redistribution of cations and enhancement in magnetic properties of sol-gel synthesized $Cu_{0.7-x}Co_xZn_{0.3}Fe_2O_4$ ($0 \leq x \leq 0.5$)," *Journal of Sol-Gel Science and Technology*, vol. 58, no. 1, pp. 70–79, 2011.

[12] S. M. Patange, S. E. Shirsath, S. S. Jadhav, K. S. Lohar, D. R. Mane, and K. M. Jadhav, "Rietveld refinement and switching properties of Cr^{3+} substituted $NiFe_2O_4$ ferrites," *Materials Letters*, vol. 64, no. 6, pp. 722–724, 2010.

[13] A. K. M. Zakaria, M. A. Asgar, S. G. Eriksson, F. U. Ahmed, S. M. Yunus, and A. K. Azad, "Preparation of Zn substituted

Ni-Fe-Cr ferrites and study of the crystal structure by neutron diffraction," *Materials Letters*, vol. 57, no. 26, pp. 4243–4250, 2003.

[14] S. M. Patange, S. E. Shirsath, B. G. Toksha, S. S. Jadhav, S. J. Shukla, and K. M. Jadhav, "Cation distribution by Rietveld, spectral and magnetic studies of chromium-substituted nickel ferrites," *Applied Physics A*, vol. 95, no. 2, pp. 429–434, 2009.

[15] B. D. Cullity, *Element of X-Ray Diffraction*, Addison-Wesley, Reading, Mass, USA, 1956.

[16] L. Weil, E. F. Bertaut, and L. Bochirol, "Propriétés magnétiques et structure de la phase quadratique du ferrite de cuivre," *Journal de Physique et Le Radium*, vol. 11, no. 5, pp. 208–212, 1950.

[17] A. Tomas, P. Laruelle, J. L. Dormann, and M. Nouges, "Structure of pentasodium dihydrogen orthophosphate diphosphate(V), $Na_5H_2(PO_4)(P_2O_7)$," *Acta Crystallographica*, vol. C39, pp. 1613–11615, 1983.

[18] K. J. Standley, *Oxide Magnetic Materials*, Clarendon Press, Oxford, UK, 1972.

[19] G. Fagherazzi and F. J. Garbassi, "X-ray diffraction measurements of the cation distributions in spinel structures," *Applied Crystallography*, vol. 5, pp. 18–23, 1972.

[20] M. U. Rana, M. Islam, and T. Abbas, "Cation distribution and magnetic interactions in Zn-substituted $CuFe_2O_4$ ferrites," *Materials Chemistry and Physics*, vol. 65, no. 3, pp. 345–349, 2000.

[21] R. D. Waldron, "Infrared spectra of ferrites," *Physical Review*, vol. 99, no. 6, pp. 1727–1735, 1955.

[22] M. A. Amer, M. A. Ahmed, M. K. El-Nimr, and M. A. Mostafa, "Mössbauer and infrared studies of the Cu–Cr ferrites," *Hyperfine Interactions*, vol. 96, no. 1, pp. 91–98, 1995.

[23] A. Shaeel and Al-Thabaiti, "Synthesis and characterization of a new cobalt polymeric spinels," *Communications de la Faculté des Sciences de l'Université d'Ankara B*, vol. 49, pp. 5–14, 2003.

[24] O. M. Hemeda, M. A. Amer, S. Aboul-Enein, and M. A. Ahmed, "Effect of sintering on X-ray and IR spectral behaviour of the $MnAl_xFe_{2-x}O_4$ ferrite system," *Physica Status Solidi (A)*, vol. 156, no. 1, pp. 29–38, 1996.

[25] E. W. Gorter, "Saturation magnetization and crystal chemistry of ferrimagnetic oxides. I. II. Theory of ferrimagnetism," *Philips Research Reports*, vol. 9, pp. 295–320, 1954.

[26] A. Pradeep, P. Priyadharsini, and G. Chandrasekaran, "Sol- gel route of synthesis of nanoparticles of $MgFe_2O_4$ and XRD, FTIR and VSM study," *Journal of Magnetism and Magnetic Materials*, vol. 320, no. 21, pp. 2774–2779, 2008.